Engineering Structures 168 (2018) 384–398

Contents lists available at ScienceDirect

Engineering Structures

journal homepage: www.elsevier.com/locate/engstruct

Theoretical analysis of reinforcement layers in bonded flexible marine hose under internal pressure

Yang Zhou[a], Menglan Duan[a,b,*], Jianmin Ma[a], Guomin Sun[c]

[a] Department of Aeronautics and Astronautics, Fudan University, Shanghai, China
[b] Institute for Ocean Engineering, China University of Petroleum, Beijing, China
[c] Offshore Oil Engineering Co., Ltd., Tianjin, China

ARTICLE INFO

Keywords:
Marine hose
Reinforcement
Theoretical

ABSTRACT

This paper portrays the results of analytical study on reinforcement layers of bonded flexible marine hose under internal pressure. Based on the anisotropic laminated composite theory, a complete theoretical solution is chosen to elaborate on the mechanical behaviour of the convoluted reinforcement layers. The developed method aims to set up a unified mathematical approach which can be suitable for arbitrary multi-layers composite of synthetic fibers in reinforcement structure. Comparative case studies are made to verify the accuracy of the method which are in agreement with the published results of four layered filament-wound composite pipe. An extended case study on a typical fourteen-layered reinforcement structure is carried out for investigating the variations of stresses and strains. Furthermore, considering the practical application in offshore engineering, parametric analysis on different known conditions, verification with experimental and numerical results are applied. Failure analysis on Tsai-Hill failure criterion are also proposed to analyze the capability of practical reinforcement layers in bonded flexible marine hose.

1. Introduction

Bonded flexible marine hose, which is frequently used in the field of offshore engineering, plays a significant role in connecting platform to shuttle tankers for oil transfer at the sea surface, see Fig. 1. A hose assembly is approximately 10–12 m in length composed of reinforced fiber, vulcanized rubber and steel end fitting. In order to present as a flexible, feasible offshore system, a marine hose is comprised of multiple layers which can provide large flexibility to withstand global bending moment and internal pressure. Since the hose is considered as bonded structure, relative displacements between various layers are not allowed due to elastomeric vulcanization, except for double carcass hoses which allow relative displacement between the carcasses. The sectional components of typical marine hose's structure is shown as follows, see Fig. 2.

The basic layers of a marine hose include carcass, liner, reinforcement layers and a steel helical wire embedded into rubber layer. Among these components in Fig. 2, reinforcement layers and steel helical wire are of vital significance. Reinforcement layers, which are also called cords or plies, are made of plentiful synthetic fibers configurated with a fixed winding angle in each layer. In a typical marine hose structure, more than 10 reinforcement layers are applied with opposite winding angles between adjoining layers [1,2]. These composite layers have many potential advantages over structures made of conventional materials. Because of highly anisotropic material properties, this kind of specific structure can resist large internal pressure and increase axial stiffness. Meanwhile, the steel wire can also guarantee the structural reinforcement by intensifying the bending stiffness of the hose and preventing its transversal section from crushing [1].

The bonded flexible marine hoses have been used in industrial sector for several decades due to well-rounded product development capabilities. However, there is a conspicuous dichotomy between industrial application and academic research. A great deal of practical issues related to scientific problems are still knotty to be clarified. Hence, in recent years, so as to verify the structural design, basic guidelines are used, such as API 17 K [3] and OCIMF [4]. Moreover, some studies have been carried out to simulate the mechanical behaviour of marine hose because of the deficiency of these guidelines, such as fatigue stress and failure analysis. Northcutt [5] developed an experimental research of bonded flexible riser, bonded flexible pipeline and bonded floating export hose. The survey showed a series of results of marine hose such as the axial and bending stiffnesses. Lassen et al. [6] proposed both experiment work and fatigue life analysis considering extreme load resistance and fatigue durability. A finite element

* Corresponding author at: Department of Aeronautics and Astronautics, Fudan University, Shanghai, China.
E-mail address: mlduan@cup.edu.cn (M. Duan).

https://doi.org/10.1016/j.engstruct.2018.04.061
Received 28 November 2017; Received in revised form 11 April 2018; Accepted 16 April 2018

Nomenclature

z	axial coordinate
θ	circumferential coordinate
r	radial coordinate
$\boldsymbol{\sigma}$	stress tensor
$\boldsymbol{\varepsilon}$	strain tensor
$\boldsymbol{u}$	displacement vector
$\boldsymbol{C}$	elastic tensor
t	tangential coordinate in local frame
b	binormal coordinate in local frame
n	normal coordinate in local frame
$\boldsymbol{C}'$	elastic tensor in local frame
ε_0	axial strain constant
γ_0	twist constant per unit length
E	elastic modulus
G	shear modulus
ν	Poisson's ratio
ϕ	winding angle

model was also built up by Lassen et al. [7] in comparison with the previous test results. Summarized of several work above, Gonzalez et al. [1] applied an analytical model [8] developed for bonded flexible pipes and proposed a numerical method based on a specific finite element model which considered continuum and rebar finite elements. Correlation between models were fine. Furthermore, Tonatto et al. [2] proposed a parametric analysis on finite element models with axisymmetric and 3D elements of a double carcass floating hose, experimental tests were also performed to validate the numerical results.

Among the limited publications in marine hoses field, it is apparently acknowledged that there are few studies concentrating on the theoretical analysis of marine hoses. The discussion could not be resolved because no one was able to answer the crucial questions in a form in which they could be pursued productively. In other words, with no decision of determining the priority of research method, the flexible marine hose, which exhibits a complex mechanical behaviour, is in need of starting from a simple question focused on its basic layers, then moving forward with a gradual research process. This will allow the feasibility of a theoretical solution and obtain credible results which can be the substantial reference for further study such as using the composite elastic theory or analytical model proposed by Batista et al. [8]. Moreover, theoretical method has its key advantage which is more efficient while implementing the parametric analysis. By contrast, although an axisymmetric model may be simple, it is still inconvenient to use finite element models to analyze parametric effects since starting a series of new calculating processes would cost more time, which is inappropriate for ongoing investigation.

Accordingly, considering all aspects mentioned above, this paper initially focuses on the mechanical behaviour of reinforcement layers, and a solution of at least 10-layered composite structure is therefore in need of taking into account. If the proposed problem can be solved analytically without excessive approximation, it can be served as a fundamental solution for further developed investigation including other layers, so as to make overall and complete comparisons with other published finite element and experimental results.

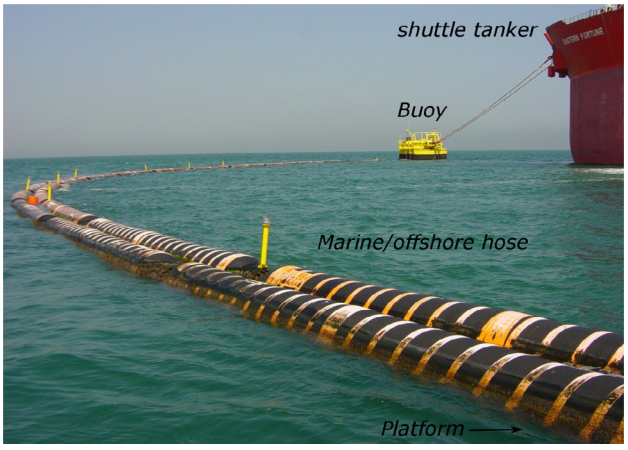

Fig. 1. Application of marine hose in offshore engineering.

In the present paper, a unified theoretical method which can be suitable for arbitrary multi-layers composite of reinforcement structures in offshore hoses is established. Based on an existing model without any modification, a pragmatic and systematic programming process of this mechanical problem is proposed in case the specific tests or studies of any appropriate *N*-layered reinforcement structure are in demand. By comparative analysis with published results, validity of the proposed analytical method is confirmed. Moreover, parametric analysis including comparison with other numerical results and failure analysis are also investigated. Since the method is implemented by a fast programming process which does not require repeating calculating processes for each parametric case, these post-processing results can be exported efficiently compared to other methods. The obtained data of reinforcement layers in offshore hoses are of paramount importance for further investigation and design in offshore engineering.

2. Model assumption & parameterization

The material status of one vulcanized reinforcement layer is presented as follows, see Fig. 3a). A typical anisotropic material structure with consistent property in only one fixed direction can be obviously observed in the figure. Since the composite elastic model can be applied in the case, it is appropriate to choose reinforcement layers as the first objective among marine hose's layers to analyze.

Considering the reinforcement structure for marine hose's geometrical model separately, this part discusses mainly the process developing from engineering structure to mathematical model. Aiming at establishing the basic mathematical foundation, it is in need of concerning all mechanical equations at appropriate local frame. Due to specific structure of bonded flexible marine hose, which enables the pipe to behave at radial and circumferential directions with an explicit physical implication, it is essential to set up a mathematical description using cylindrical coordinate system. The diagrammatic sketch from engineering model to mathematical parameterization can be demonstrated as follows, see Fig. 3b).

In such a context, what is recognized as a cylindrical model can be validated in the following definition:

A subset $\Sigma \subset \mathbb{R}^3$ is a regular surface, if there establishes a map, satisfying the following form

$$\boldsymbol{\Sigma}(\boldsymbol{x}_\Sigma)\colon \mathbb{R}^3 \ni \boldsymbol{x}_\Sigma = \begin{bmatrix} z \\ \theta \\ r \end{bmatrix} \mapsto \boldsymbol{\Sigma}(\boldsymbol{x}_\Sigma) = \begin{bmatrix} z = z \\ y = r\cdot\sin\theta \\ x = r\cdot\cos\theta \end{bmatrix} \in \mathbb{R}^3 \tag{1}$$

where (z,θ,r) is local cylindrical frame while (z,y,x) represents the standard orthogonal basis. The vector form $\boldsymbol{\Sigma}(\boldsymbol{x}_\Sigma) = (z(z,\theta,r),y(z,\theta,r),x(z,\theta,r))$ can be used conveniently to study differential and integral calculus on the surface. Furthermore, it is emphasized here that the sequence of coordinate is deliberately designed using right-hand rule corresponding to another local frame (t,b,n) which will be introduced later.

With establishment of local frame on the layers's surface, then mechanical analysis can be implemented from its vectorial form.

Note that, throughout the past decade, some studies have been

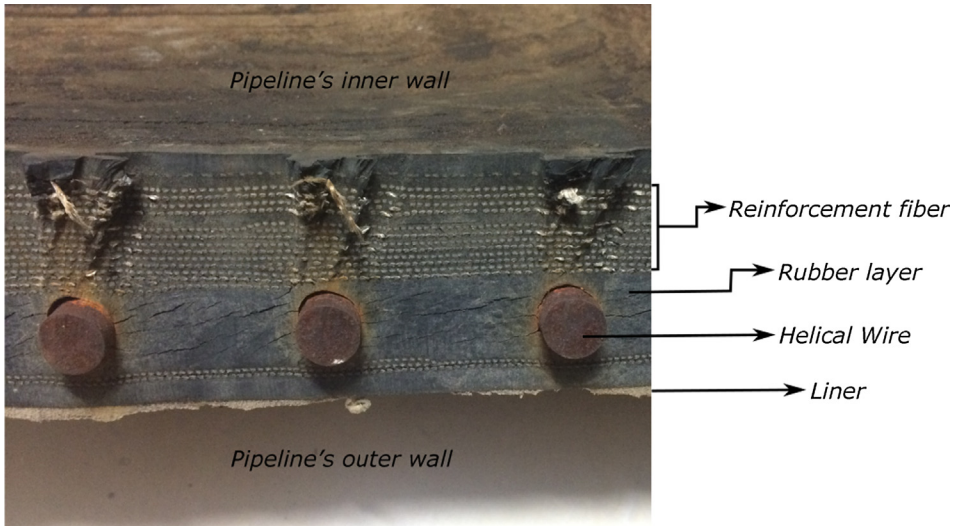

Fig. 2. Sectional components of typical marine hose's structure.

carried out in composite structure field dealt with analysis of filament-wound fiber-reinforced composite pipe. The mechanical behaviour has a noteworthy affinity with that of reinforcement layers in bonded flexible marine hose. The structure is based on laminated anisotropic composites, which can possess a transversely isotropic property at the winding angle. Rosenow [9] discussed the stress and strains of filament wound pipe with consideration of wind angle effects, which including a range from 15° to 85°. Based on theory of elasticity of anisotropic bodies, Wild and Vickers [10] developed an analytical prediction to assess the mechanical behaviour of filament-wound structure under several loading conditions such as axial and centrifugal forces. Moreover, buckling behaviour of multi-layered composite cylindrical shells was studied by Smerdov [11,12], axial compression and external pressure which represent two different boundary conditions are considered in the two papers. These studies established the classical procedure of analytical research on laminated anisotropic composite pipe.

Meanwhile, Xia et al. [13,14] proposed a theoretical approach to analysis the filament-wound composite pipe predicated on the fundamental system of equations in mechanics of elasticity, and then Takayanagi et al. [15] presented the prediction of failure strength of a filament-wound pipe based on a maximum stress failure criterion. In addition, Ansari et al. [16] made a progress in changing the condition load to cyclic internal pressure and cyclic temperature. It is emphasized that, due to sophisticated interactions between adjacent filament-wound layers, the complexity of system will gather significant accretions exponentially with the number of layers increased. In view of this, Xia et al. [13] only dealt with a case study of four-layered filament-wound composite pipe. Other authors such as [17,18] sought for progressive research mainly on changing boundary conditions or concentrating on variations of the winding angle, not on considering the structural influence with respect to a more layers structure case.

Hence, based on previous study of filament-wound fiber-reinforced composite pipes, it is promising to develop a totally theoretical method for reinforcement layers of marine hose under a given boundary condition. Considering that, the implementation method raised by Xia et al. [13] is deficient to solve a general problem when the number of layers increases since only a description for the scale of N-layered equations system is given in the paper, which allows anyone to use it. In order to meet the practical demand in engineering, a systematic approach based on Xia et al.'s existing model [13] which can be suitable for any multiple numbers of reinforcement layers is the prior task. The inheritance and development between adjacent reinforcement layers are accompanied by certain regularity and will be detailed introduced in this paper.

3. Preliminaries

The preliminaries part includes several basic assumptions and equations of the mechanical system. Note that, some are presented in previous published papers, such as Xia et al. [13] and Ansari et al. [16].

a) b)

Fig. 3. Structure and parameterization of reinforcement layers.

More references related to the mathematical and mechanical structure can be found in treatises [19,20]. However, these equations presented below are fundamental and cannot be eliminated since the integrity of the whole discussion may be vitiated.

It starts from some essential assumptions of this specific mechanical structure, and put forward the system of equations by constitutive relation and strain, stress analysis. Meanwhile, because of the regularity of this anisotropic material, mechanical simplifications of the elastic coefficient are also demonstrated. Finally, in order to simulate the most likely working condition of bonded flexible marine hose, internal pressure is chosen as boundary conditions to study the mechanical problem. Bending is also a common working condition in the case. However, it is advisable to analyze only one condition first to see the possibility of mixed working conditions in further extended investigation.

3.1. Model restrains

As is shown in Fig. 3b), a typical reinforcement layer is made up of several composite laminate with a given winding angle ϕ. When pipe is subjected to axisymmetric load such as internal pressure, the stresses and strains are independent of θ, namely,

$$\frac{\partial \boldsymbol{u}}{\partial \theta} = 0, \quad \frac{\partial \boldsymbol{\sigma}}{\partial \theta} = 0, \quad \frac{\partial \boldsymbol{\varepsilon}}{\partial \theta} = 0 \tag{2}$$

where $\boldsymbol{u}$,$\boldsymbol{\sigma}$ and $\boldsymbol{\varepsilon}$ represent displacement vector, stress tensor and strain tensor, respectively. The components of each quantity in matrix form along local coordinates z,θ and r are as follows:

$$\boldsymbol{u} = [u_z,u_\theta,u_r], \quad \boldsymbol{\sigma} = \begin{bmatrix} \sigma_z & \tau_{z\theta} & \tau_{zr} \\ \tau_{\theta z} & \sigma_\theta & \tau_{\theta r} \\ \tau_{rz} & \tau_{r\theta} & \sigma_r \end{bmatrix}, \quad \boldsymbol{\varepsilon} = \begin{bmatrix} \varepsilon_z & \varepsilon_{z\theta} & \varepsilon_{zr} \\ \varepsilon_{\theta z} & \varepsilon_\theta & \varepsilon_{\theta r} \\ \varepsilon_{rz} & \varepsilon_{r\theta} & \varepsilon_r \end{bmatrix} \tag{3}$$

Note that, $\tau_{z\theta} = \tau_{\theta z}$,$\tau_{zr} = \tau_{rz}$ and $\tau_{\theta r} = \tau_{r\theta}$ denote shear stresses. $\varepsilon_{z\theta} = \varepsilon_{\theta z} = \frac{1}{2}\gamma_{z\theta}$,$\varepsilon_{zr} = \varepsilon_{rz} = \frac{1}{2}\gamma_{zr}$ and $\varepsilon_{\theta r} = \varepsilon_{r\theta} = \frac{1}{2}\gamma_{\theta r}$ are tensorial shear strains. Where $\gamma_{z\theta}$,γ_{zr} and $\gamma_{\theta r}$ represent engineering shear strains. These mechanical quantities will be used in next several parts.

Moreover, the plate strain assumption can be applicable in this case since the dimension along z – coordinate is more significant than the rest two dimensions, then the radial and axial displacements are independent along axial and radial directions respectively. The displacements $\boldsymbol{u}$ will be restrained and expressed as the following form.

$$u_z = u_z(z), \quad u_\theta = u_\theta(r,z), \quad u_r = u_r(r) \tag{4}$$

It is noted that here each composite laminate layer exhibit identical mechanical property. The following system of equations can be applied in every laminate layer except for the difference of winding angles and boundary conditions.

3.2. Basic mechanical equations

Constitutive relation and strain, stress equations are listed as follows:

$$\begin{bmatrix} \sigma_z \\ \sigma_\theta \\ \sigma_r \\ \tau_{\theta r} \\ \tau_{zr} \\ \tau_{z\theta} \end{bmatrix} = \boldsymbol{C} \begin{bmatrix} \varepsilon_z \\ \varepsilon_\theta \\ \varepsilon_r \\ \gamma_{\theta r} \\ \gamma_{zr} \\ \gamma_{z\theta} \end{bmatrix} = \begin{bmatrix} C_{11} & C_{12} & C_{13} & 0 & 0 & C_{16} \\ C_{12} & C_{22} & C_{23} & 0 & 0 & C_{26} \\ C_{13} & C_{23} & C_{33} & 0 & 0 & C_{36} \\ 0 & 0 & 0 & C_{44} & C_{45} & 0 \\ 0 & 0 & 0 & C_{45} & C_{55} & 0 \\ C_{16} & C_{26} & C_{36} & 0 & 0 & C_{66} \end{bmatrix} \begin{bmatrix} \varepsilon_z \\ \varepsilon_\theta \\ \varepsilon_r \\ \gamma_{\theta r} \\ \gamma_{zr} \\ \gamma_{z\theta} \end{bmatrix} \tag{5}$$

$$\varepsilon_z = \frac{\mathrm{d}u_z}{\mathrm{d}z}, \quad \varepsilon_\theta = \frac{u_r}{r}, \quad \varepsilon_r = \frac{\mathrm{d}u_r}{\mathrm{d}r}$$
$$\gamma_{zr} = 0, \quad \gamma_{\theta r} = \frac{\partial u_\theta}{\partial r} - \frac{u_\theta}{r}, \quad \gamma_{z\theta} = \frac{\partial u_\theta}{\partial z} \tag{6}$$

$$\frac{\mathrm{d}\sigma_r}{\mathrm{d}r} + \frac{\sigma_r - \sigma_\theta}{r} = 0 \tag{7}$$

$$\frac{\mathrm{d}\tau_{\theta r}}{\mathrm{d}r} + \frac{2\tau_{\theta r}}{r} = 0 \tag{8}$$

$$\frac{\mathrm{d}\tau_{zr}}{\partial r} + \frac{\tau_{zr}}{r} = 0 \tag{9}$$

Note that, elastic tensor $\boldsymbol{C}$ is a fourth-order tensor with 21 different components under anisotropic condition. According to the case, it can be seen that there exists only one elastic axisymmetric plane (along r-axial), the number of the elastic components is therefore reduced from 21 to 13. Eq. (6) is also a simplified form by Eqs. (2) and (4) from original componentwise strain equation.

Meanwhile, body force in Eqs. (7)–(9) is negligible since it is assumed to be balanced with buoyancy.

From Eqs.)(5)–(9), the elastic problem with apropos boundary conditions can be solved theoretically. This formulation of the elastic equations has the advantage that, although the exact nonlinear partial differential equations are maintained, with practical restrains of structure and specific boundary conditions the complex system can be dealt with in appropriate simplification.

3.3. Mechanical simplifications

In order to obtain the laminate surface properties, and considering that they form a specific regularity that the material is orthotropic along winding angle, it is emphasized that another local frame (t,b,n) is essential to be set up. It can be seen here, if let the tangential coordinate as the first place, with a certain rotation of local frame, the sequence of cylindrical coordinates can only be (z,θ,r).

The relation between the two local frames can be seen in the following figure, see Fig. 4.

Along the local frame (t,b,n), elastic quantities will reduce to 9, and can be defined as modulus of elasticity and shearing, and Poison ratio: E_t,E_b,E_n,ν_{tb},ν_{nt},ν_{nb},G_{tt},G_{bb},G_{nn}.

In addition, it is noted that the same behaviour along b-axis and n-axis is qualified in the elasticity. Hence, orthotropic elasticity can be simplified to plane orthotropic elasticity – the elastic quantities will reduce again to 4 with the following relations:

$$E_b = E_n, \quad G_{bb} = G_{nn}, \quad \nu_{nt} = \nu_{bt} \tag{10}$$

These three coefficients satisfy the following relation,

$$G_{tt} = \frac{E_b}{2(1 + \nu_{nb})} \tag{11}$$

With the simplified definition, the modified constitutive relation can be expressed under (t,b,n) frame.

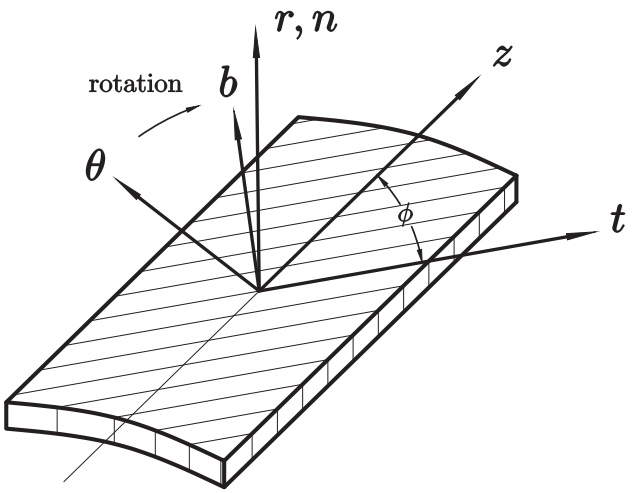

Fig. 4. Transformation of two coordinates.

$$\begin{bmatrix}\varepsilon_t\\ \varepsilon_b\\ \varepsilon_n\\ \gamma_{bn}\\ \gamma_{nt}\\ \gamma_{tb}\end{bmatrix}=\begin{bmatrix}\frac{1}{E_t} & -\frac{\nu_{bt}}{E_t} & -\frac{\nu_{bt}}{E_t} & 0 & 0 & 0\\ & \frac{1}{E_b} & -\frac{\nu_{nb}}{E_b} & 0 & 0 & 0\\ & & \frac{1}{E_n} & 0 & 0 & 0\\ & & & \frac{1+\nu_{bn}}{E_b} & 0 & 0\\ & & Sym. & & \frac{1+\nu_{nt}}{E_n} & 0\\ & & & & & \frac{1+\nu_{tb}}{E_t}\end{bmatrix}\begin{bmatrix}\sigma_t\\ \sigma_b\\ \sigma_n\\ \tau_{bn}\\ \tau_{nt}\\ \tau_{tb}\end{bmatrix} \tag{12}$$

Note that, in practical engineering, when using the shear modulus G, the definition of strain is twice the value of that in Eq. (12). Then if this elastic coefficient matrix is defined as $\boldsymbol{C}' = [C'_{ij}]$, it can be obtain by,

$$[C'_{ij}]=\begin{bmatrix}\frac{1}{E_t} & -\frac{\nu_{bt}}{E_t} & -\frac{\nu_{bt}}{E_t} & 0 & 0 & 0\\ & \frac{1}{E_b} & -\frac{\nu_{nb}}{E_b} & 0 & 0 & 0\\ & & \frac{1}{E_n} & 0 & 0 & 0\\ & & & \frac{1}{G_{tt}} & 0 & 0\\ & & Sym. & & \frac{1}{G_{bb}} & 0\\ & & & & & \frac{1}{G_{nn}}\end{bmatrix}^{-1} \tag{13}$$

It is apparently seen that a rotation relation is established between $\boldsymbol{C}$ and $\boldsymbol{C}'$, if define

$$[C'_{ij}] = [C'_{11},C'_{22},C'_{33},C'_{12},C'_{13},C'_{23},C'_{44},C'_{55},C'_{66}]^T \tag{14}$$

$$[C_{pj}] = [C_{11},C_{12},C_{13},C_{16},C_{22},C_{23},C_{26},C_{33},C_{36},C_{44},C_{45},C_{55},C_{66}]^T \tag{15}$$

Then,

$$[C_{pj}] = [A_{pi}][C'_{ij}] \tag{16}$$

$[A_{pi}]$ is a rotation matrix which can be calculated as the form presented in Appendix.

3.4. Boundary conditions

All equations mentioned above are subjected to practical condition and the problem will have access to a theoretical solution by a given boundary condition. This paper deals with the condition under constant internal pressure which is the most common working condition in bonded flexible marine hoses. Considering a N – layered laminate composite of reinforcement layers, given the constant internal pressure p_0, the boundary conditions can be listed as follows:

$$\sigma_r^{(1)}(r_0) = -p_0, \quad \sigma_r^{(N)}(r_N) = 0 \tag{17}$$

$$\tau_{\theta r}^{(1)}(r_0) = \tau_{zr}^{(1)}(r_0) = 0, \quad \tau_{\theta r}^{(N)}(r_N) = \tau_{zr}^{(N)}(r_N) = 0 \tag{18}$$

Where r_0 is the inner radius of the first layer of plies, and r_k $(k = 1,...,N)$ represents the upper radius of each layer. Note that, to separate with some symbols of arithmetical operations, superscript (k) on expressions of stresses and strain also means quantities of "the k layer".

Since adjacent layers of plies in marine hose are completely bonded, namely, the outer radius of k – layer equals to the inner radius of $k+1$ – layer, this phenomena will generate the following relations,

$$u_r^{(k)}(r_k) = u_r^{(k+1)}(r_k), \quad \sigma_r^{(k)}(r_k) = \sigma_r^{(k+1)}(r_k) \tag{19}$$

Considering the global equilibrium analysis of marine hose, it is noted that the forces distributed on the two end fitting equal to the inner force of pipe along z – axial, this leads to the following integral equation:

$$2\pi\sum_{k=1}^{n}\int_{r_{k-1}}^{r_k}\sigma_z^{(k)}(r)r\mathrm{d}r = \pi r_0^2 p_0 \tag{20}$$

The global pipe exhibits no torsion because of the axisymmetric loading, then,

$$2\pi\sum_{k=1}^{n}\int_{r_{k-1}}^{r_k}\tau_{z\theta}^{(k)}(r)r^2\mathrm{d}r = 0 \tag{21}$$

4. Theoretical analysis

If the pipe is subjected to constant internal pressure, resultant force acting on axial direction is functionally equivalent to constant tension which will lead to constant axial strain, then displacement along z – axial u_z can be calculated from Eq. (6),

$$\varepsilon_z = \frac{\mathrm{d}u_z}{\mathrm{d}z} = \varepsilon_0, \quad u_z(z) = \varepsilon_0 z \tag{22}$$

where ε_0 denotes the axial strain, which is a constant when the pipe suffers a given internal pressure.

Eqs. (8) and (9) can be solved theoretically with the following results:

$$\tau_{\theta r} = \frac{\mathscr{C}_1}{r^2}, \quad \tau_{zr} = \frac{\mathscr{C}_2}{r} \tag{23}$$

$\mathscr{C}_1, \mathscr{C}_2$ are unknown integration constants.

Substituting Eqs. (17) and (18) into Eq. (23), the above two integration constants will be zero: $\mathscr{C}_1 = \mathscr{C}_2 = 0$. Combining Eqs. (6) and constitutive relation (5), the following result can be obtained:

$$\gamma_{\theta r} = \frac{\partial u_\theta}{\partial r} - \frac{u_\theta}{r} = -\frac{C_{55}}{(C_{45})^2 - C_{44}C_{55}}\frac{\mathscr{C}_1}{r^2} + \frac{C_{45}}{(C_{45})^2 - C_{44}C_{55}}\frac{\mathscr{C}_2}{r} = 0 \tag{24}$$

Therefore, u_θ forms a linear function with respect to r. Considering partial derivative of u_θ with respect to z exhibits a physical implication of twisting, displacement along θ – axis u_θ can be obtained also from Eq. (6):

$$\gamma_{z\theta} = \frac{\partial u_\theta}{\partial z} = \gamma_0 r, \quad u_\theta(r,z) = \gamma_0 r z \tag{25}$$

γ_0 is a physical quantity which represents twist of the surface per unit length.

Substituting Eq. (5) into simplified stress relation Eq. (7), and using Eq. (6), a differential equation about displacement along r – axis u_r with respect to r can be obtained in the following form:

$$\frac{\mathrm{d}^2u_r}{\mathrm{d}r^2} + \frac{1}{r}\frac{\mathrm{d}u_r}{\mathrm{d}r} - \frac{C_{22}/C_{33}}{r^2}u_r = \frac{C_{12}-C_{13}}{C_{33}}\frac{\varepsilon_0}{r} + \frac{C_{26}-2C_{36}}{C_{33}}\gamma_0 \tag{26}$$

It is of vital significance to emphasized that this second-order linear differential equation can be solved analytically and with no need to seek for a numerical solution. Firstly, considering the specific mathematical structure of Eq. (26) with variable coefficients $1/r$ and $1/r^2$ of terms in the left side and based on an indeterminate coefficient method, if defining

$$\alpha = \sqrt{C_{22}/C_{33}} \tag{27}$$

then r^α and $r^{-\alpha}$ will be obtained as the fundamental system of solutions of the homogeneous linear differential equation corresponding to Eq. (26). Namely, r^α and $r^{-\alpha}$ are two special linearly independent solutions of the following equation:

$$\frac{\mathrm{d}^2u_r}{\mathrm{d}r^2} + \frac{1}{r}\frac{\mathrm{d}u_r}{\mathrm{d}r} - \frac{\alpha^2}{r^2}u_r = 0 \tag{28}$$

Therefore, the only task is to find a special solution for Eq. (28). Note that, apart from the constants such as C,ε_0 and γ_0, the only variable coefficient of Eq. (28) in the right side is $1/r$. It is apposite also to construct a polynomial to obtain the special solution $\overline{u_r}$, let

$$\overline{u_r}(r) = \omega_1 r^2 + \omega_2 r + \omega_3 \tag{29}$$

Substituting Eq. (29) into Eq. (26), then

$$\omega_1 = \frac{C_{26}-2C_{36}}{4C_{33}-C_{22}}\cdot\gamma_0 \tag{30}$$

$$\omega_2 = \frac{C_{12}-C_{13}}{C_{33}-C_{22}}\cdot\varepsilon_0 \tag{31}$$

$$\omega_3 = 0 \tag{32}$$

Since ε_0 and γ_0 are unknown quantities that need to be calculated, here two known quantites $\beta_1 = \omega_1/\gamma_0$ and $\beta_2 = \omega_2/\varepsilon_0$ are used to replace ω_1 and ω_2. Hence,

$$\overline{u_r}(r) = \beta_1\gamma_0 r^2 + \beta_2\varepsilon_0 r \tag{33}$$

To sum up, the final general solution of Eq. (26) is written as,

$$u_r(r) = \mathscr{A}\cdot r^{\alpha} + \mathscr{B}\cdot r^{-\alpha} + \overline{u_r} = \mathscr{A}\cdot r^{\alpha} + \mathscr{B}\cdot r^{-\alpha} + \beta_1\gamma_0 r^2 + \beta_2\varepsilon_0 r \tag{34}$$

where $\mathscr{A}$ and $\mathscr{B}$ are integration constants.

If three displacements u_z,u_θ and u_r can be calculated by Eqs. (22), (25) and (34), then all unknown quantities of the system can be obtained through stress, strain and constitutive relations. Since the only differential equation in the system is Eq. (28) which has a general solution, the method provided in the paper is analytical.

5. Solution

For N – layered composite ply, there are $2N + 2$ unknown quantities: $\mathscr{A}^k$ $(k = 1,2,...,N)$,$\mathscr{B}^k$ $(k = 1,2,...,N)$ and ε_0,γ_0. Eqs. (17) and (19) will generate $2N$ equations corresponding to σ_r and u_r:

$$\begin{aligned}
&\sigma_r^{(1)}(r_0) = -p_0\\
&u_r^{(k)}(r_k) - u_r^{(k+1)}(r_k) = 0, \quad k = 1,...,N-1\\
&\sigma_r^{(k)}(r_k) - \sigma_r^{(k+1)}(r_k) = 0, \quad k = 1,...,N-1\\
&\sigma_r^{(N)} = 0
\end{aligned} \tag{35}$$

Eqs. (20) and (21) will furnish the rest 2 equations.

Thus far, Eqs. (35), (20) and (21) provide the crude form of equation system which is the key solver in this model. If N is not large, such as 1 or 2, it can be clearly seen that fundamental operations of arithmetic is enough to solve the problem. That is why Xia et al. [13] chose a 4-layered pipe to perform the case study. However, Eq. (35) exhibits an exceptional unity of equation form which can be used as a function while the independent variable is k. Then, a list of relative equations can be summarized as a whole which is not mentioned in [13]. Eqs. (20) and (21) can be also dealt with by specially appointed setting and computation. Therefore, an extended generalized method can be established by means of programming ideas such as loop and condition, the unified implementation can be easily applied to practical problems of any multi-layered reinforcement structure under internal pressure.

Note that, constant pressure is a prerequisite for Eqs. (22) and (25). Change of these two equations may also change the final solver. Therefore, it is not easy to cover dynamic load in the present method. This would be a further investigation since there are also many other conditions for offshore hose.

For simplicity, combined by Eqs. (35), (20) and (21), it is noteworthy to establish a matrix form of formulas as follows:

$$\boldsymbol{\Omega}\cdot\begin{bmatrix}\mathscr{A}^{(1)}\\ \mathscr{A}^{(2)}\\ \vdots\\ \mathscr{A}^{(N)}\\ \mathscr{B}^{(1)}\\ \mathscr{B}^{(2)}\\ \vdots\\ \mathscr{B}^{(N)}\\ \varepsilon_0\\ \gamma_0\end{bmatrix} = \begin{bmatrix}-p_0\\ 0\\ \vdots\\ 0\\ 0\\ 0\\ \vdots\\ 0\\ \frac{r_0^2 p_0}{2}\\ 0\end{bmatrix} \tag{36}$$

where

$$\boldsymbol{\Omega} = [\boldsymbol{A}\ \ \boldsymbol{B}\ \ \boldsymbol{\Lambda}] \tag{37}$$

Note that, $\boldsymbol{\Omega}$ is a matrix with dimension of $(2N + 2) \times (2N + 2)$. Detailed expressions of $\boldsymbol{A}$,$\boldsymbol{B}$ and $\boldsymbol{\Lambda}$ are,

$$\boldsymbol{A} = \begin{bmatrix}
a_{11} & 0 & ... & 0\\
a_{21} & a_{22} & & \vdots\\
\vdots & \ddots & \ddots & 0\\
0 & ... & a_{N(N-1)} & a_{NN}\\
a_{(N+1)1} & a_{(N+1)2} & ... & 0\\
0 & \ddots & \ddots & \vdots\\
\vdots & & a_{(2N-1)(N-1)} & a_{(2N-1)N}\\
0 & ... & 0 & a_{(2N)N}\\
a_{(2N+1)1} & a_{(2N+1)2} & ... & a_{(2N+1)N}\\
a_{(2N+2)1} & a_{(2N+2)2} & ... & a_{(2N+2)N}
\end{bmatrix} \tag{38}$$

$$\boldsymbol{B} = \begin{bmatrix}
b_{11} & 0 & ... & 0\\
b_{21} & b_{22} & & \vdots\\
\vdots & \ddots & \ddots & 0\\
0 & ... & b_{N(N-1)} & b_{NN}\\
b_{(N+1)1} & b_{(N+1)2} & ... & 0\\
0 & \ddots & \ddots & \vdots\\
\vdots & & b_{(2N-1)(N-1)} & b_{(2N-1)N}\\
0 & 0 & ... & b_{(2N)N}\\
b_{(2N+1)1} & b_{(2N+1)2} & ... & b_{(2N+1)N}\\
b_{(2N+2)1} & b_{(2N+2)2} & ... & b_{(2N+2)N}
\end{bmatrix} \tag{39}$$

$$\boldsymbol{\Lambda} = \begin{bmatrix}
\lambda_{11} & \lambda_{12}\\
\lambda_{21} & \lambda_{22}\\
\vdots & \vdots\\
\lambda_{(N-1)1} & \lambda_{(N-1)2}\\
\lambda_{N1} & \lambda_{N2}\\
\lambda_{(N+1)1} & \lambda_{(N+1)2}\\
\lambda_{(N+2)1} & \lambda_{(N+2)2}\\
\vdots & \vdots\\
\lambda_{(2N)1} & \lambda_{(2N)2}\\
\lambda_{(2N+1)1} & \lambda_{(2N+1)2}\\
\lambda_{(2N+2)1} & \lambda_{(2N+2)2}
\end{bmatrix} \tag{40}$$

Where parameters a_{ij},b_{ij} and λ_{ij} are detailed calculated by Eqs. (35), (20) and (21), and all expressions of these parameters are listed in Appendix. With all formulas provided above, a new generalized method for N – layered composite plies is established. Unknown quantities $\mathscr{A}$,$\mathscr{B}$,ε_0 and γ_0 will be obtained by solving the matrix-algebraic equations corresponding to each layer. Then substituting these results into Eqs. (34), (25) and (22), three displacements u_r,u_θ,u_z will be given, the rest mechanical quantities can be also calculated completely by Eqs. (5) and (6). The method carried out in the paper is a totally analytical study without any approximation and will be convincingly verified while evaluating the validity of this solution.

6. Detailed explication of the established method

6.1. Calculating process

Considering that the mechanical problem depicts an implicit process, calculating implementation is therefore manifested in the following flowchart for convenience, see Fig. 5.

Firstly, with all known quantities such as material constants E,G,ν and winding angle ϕ for each layer, the elastic coefficient $\boldsymbol{C}$ will be given. Then according to corresponding equations, matrix $\boldsymbol{\Omega}$ can be determined. With all given quantities like α,β_1,β_2 and boundary condition p_0, the key process is to solve Eq. (36), this will lead to the results of $\mathscr{A}$,$\mathscr{B}$,ε_0,γ_0 for each layer. If the four quantities can be calculated correctly, all mechanical results will be totally obtained.

Although the system of equations is huge and complex, with

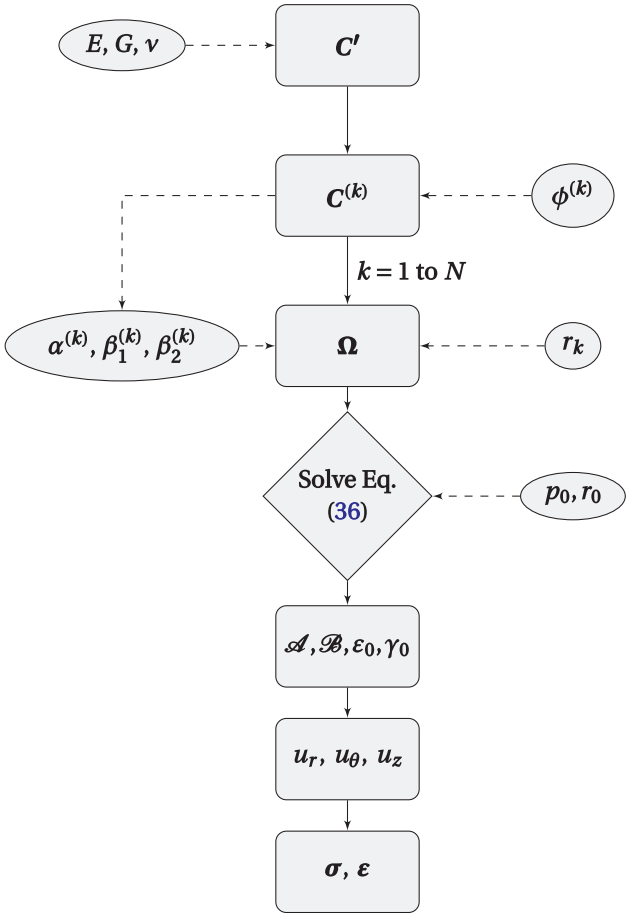

Fig. 5. Flowchart of the calculating process.

assistance of computation programming calculating process can be implemented automatically under initialized function specification.

6.2. Distinctions and advantages

Although the main theoretical method is fairly illustrated so far, there are still some points that are necessary to be elaborated further.

Firstly, the paper initially aims at solving an engineering problem corresponding to bonded flexible marine hose in offshore field. The key objective is marine hose instead of only an extended study of filament-wound fiber-reinforced composite pipes. If the task is only a "4-layered structure to *N*-layered structure" study, the main contribution would be the research on mathematical formulation. In order to solve a real engineering problem of the reinforcement layers in marine hose, a more than 4-layered model is indeed in demand, other than a basic mathematical interest of studying the multi-layered structure and finding its intrinsic link between layers. Hence, all results obtained by the method is in the service of offshore engineering. Although the method proposed now cannot obtain results including other layers such as steel coil which is hard to make comparison with other FE models, it can still provide substantial reference for further validation and calibration of modified bonded flexible marine hose.

Secondly, the paper proposes a significant programming idea of this mechanical problem which is not given by Xia et al. [13] and many other authors. In practical application, a finished programming code can be suitable for any *N*-layered case with little modification. For instance, considering a 4-layered ply, when defining some items such as the elements in $\boldsymbol{A}$, functions and loops can be applicable easily to guarantee the integrity of computational process.

In the Mathematica programming code presented in Fig. 6, for convenience the elastic tensor $\boldsymbol{C}$ is defined as a column vector function $c[k]$ while $c[k][i,j]$ represents the element of $c[k]$, then with definitions of coefficient $\alpha[k]$ and the fourth expression of elements in matrix $\boldsymbol{A}$ (see Appendix), the values of $a_{(N+1)1}, a_{(N+2)2}, \ldots, a_{(2\times N)N}$ can be defined by a loop. In a 4 – layered case, only four elements are defined: $a_{(4+1)1}, a_{(4+2)2}, a_{(4+3)3}, a_{(2\times 4)4}$. Therefore, it is easy to list all expressions one by one. However, in a *N* – layered case, the loop idea is of vital significance. Likewise, the other elements can be also assigned by similar operations.

It is also accessible to obtain the final results of $\mathscr{A}, \mathscr{B}, \varepsilon_0, \gamma_0$ straightforwardly. All information of results can be included in a column vector by one statement. Therefore, the data of $\mathscr{A}, \mathscr{B}, \varepsilon_0, \gamma_0$ can be extracted by a loop structure.

The advantage is that, when another multi-layered case study is in demand, by changing the value 4 in number *N* to the objective number, the programming will function quickly to bring out the results.

Finally, this paper raises a crucial question about the mechanical model: what it will be like when the number of reinforcement layers increases. The tendencies of stress and strain changes still remain uncertain. It still puzzles many authors that whether the 14-layered reinforcement structure is secure enough to guarantee the essential strength and stiffness condition in ocean engineering application. By means of the generalized theoretical method, more new results can be obtained such as parametric analysis on different internal pressures, winding angles and even different number of layers in a unified programming process. The numerical methods, such as FEM, they can also determine the stiffness of each layer of plies efficiently. However, the

```
...
alpha[k_] := (c[k][[5, 1]]/c[k][[8, 1]])^(1/2);
a4[k_] := (c[k][[6, 1]] + alpha[k] c[k][[8, 1]]) r[k]^(alpha[k] - 1);
...
N = 4
bmA = Table[0, {i, 2*N + 2}, {j, N}]

i = N + 1;
  While[i <= 2*N,
    For[j = i - N, j <= i - N,
      bmA[[i, j]] = a4[j];
        j++
    ];
    i++
  ];
bmA
```

Fig. 6. Mathematica programming code for the proposed method.

parametric results such as the mechanical quantities corresponding to different number of layers cannot be obtained after only one calculating process. The values of stresses and strains of the multi-layered reinforcement structure in bonded flexible marine hose can serve as a reliable prediction for further offshore industry, like failure analysis. The following several parts will demonstrate these aspects in order to observe the strength of the proposed method in multiple perspectives.

7. Case studies

7.1. Controlled analysis

To verify the proposed theoretical method, it is reliable to make comparisons with published results. Since the method presented in the paper is illuminated by a study of four-layered filament-wound composite pipes under internal pressure, it is emphasized to make a case-control study with $N = 4$. The known quantities including size and material constants are given by Xia et al. [13] and listed in Tables 1 and 2.

It is note that winding angles in original paper of Xia et al. [13] are provided in three types of fiber orientation groups. Here since + 55/−55 is a typical type in marine hoses, this only control group of opposite fiber orientation (+ 55/−55) is studied.

Fig. 7 shows the result of displacement along radial direction with respect to radial coordinate. The expression of u_r is a key foundation which can assist to export the rest mechanical quantities. From the figure, it can be seen that displacement u_r begins with approximate 0.1800 mm, decrease slowly to 0.1766 mm which stops corresponding to outer radius of the pipe. The result is nearly the same as that in Xia et al. [13].

Fig. 8 describes both circumferential and axial stresses along radius of pipe. Both the two kinds of stresses exhibit a little discontinuous phenomenons when the radius move to the conjunctions of adjacent layers, both have a tendency to decrease slightly with respect to radius. Moreover, it is clear that the ± 55° winding angles are proved to be the optimum angles assemble for a filament wound composite pipe with a circumferential-axial stress ratio of 2: 1, which is also demonstrated in [13,15].

As is shown in Fig. 9, radial stress increase from $-p_0$ internal pressure which is the boundary condition of the presented system, and stops at 0 MPa. Note that, the figure also exhibits a little discontinuity at several points corresponding to the conjunctions of adjacent layers. Theoretically, this phenomenon is not allowed due to Eq. (19). However, after a deep exploration of the original data, it shows that the deviation is caused by computational error which is hard to eliminated in Mathematica programming. Since it is not the main factor to the final results, the deviation is retained here to represent the authenticity of original results.

Fig. 10 portrays shear stress $\tau_{z\theta}$ along radius of the pipe. The result shows a unique difference from normal stresses. The magnitude of $\tau_{z\theta}$ is around 165 MPa and sign alternates with respect to relative winding angle.

The results mentioned above are in agreement with those in Xia et al. [13]. Note that, since the comparative results are fairly closed, it is not easy to observe everything in detail, the corresponding two comparative curves are therefore not portrayed in one figure. However, Table 3 lists all compared results. The values of displacements and stresses are extracted from the beginning of the curves respectively, since decreases of these curves are not violet and inconsequential compared to the former. From Table 3, it can be concluded that, based on the existing model without any modification, the results coincide exactly with Xia et al.'s results.

7.2. Extended analysis

Since a controlled analysis is verified, it is convincing to implement an extended analysis which enables the fundamental data of a 14-layered reinforcement structure. Based on previous demonstration, let $N = 14$, and a series of same known quantities are considered in order to summarize the relevance of both cases more clearly: inner radius $r_0 = 50$ mm with each ply thickness of 0.5 mm, the outer radius which is the external radius of the fourteenth layer would be $r_0 + 14 \times 0.5 = 57$ mm. Same material constants and boundary conditions are applied, then the following corresponding results are therefore obtained.

Compared to Fig. 7, the new 14 layers displacement u_r in Fig. 11 depicts a less magnitude. In Fig. 12, circumferential stress decreases from 270 MPa to 80 MPa, while axial stress decreases from 118 MPa to 34 MPa. However, a circumferential-axial stress ratio of 2:1 is still satisfied. All results concerned above are eligible to reveal a conclusion that strength of the structure can be enhanced efficiently by increasing the number of layers.

The radial stress is still in accordance with boundary condition which is $-p_0$ and 0 in internal and external of the pipe respectively, see Fig. 13. It is meaningful to analyze the results in Fig. 14. When the number of layers varies, shear stress is accompanied by certain regularity. The variation of sign remains, magnitude in the beginning also decreases as same as those of other stresses. However, a tendency of shear stress's convergency which cannot be apparently observed in Fig. 10 occurs in scenario of 14-layered reinforcement structure. It is emphasized to summarize the alleviation of shear stress with respect to radius of the pipe. Namely, it can be summarized that, interactions between layers which are represented typically as shear forces attenuates in pace with the increase of pipe's radius.

It is noted here, since in a typical marine hose structure, 14 reinforcement layers are applied with opposite winding angles between adjoining layers, the paper only includes an extended case study of 14 layers. However, the method is generic, based on the theoretical method, the upper limit of layer number is infinite. The only limitation is the plate strain assumption, which means that the dimension along z – coordinate is more significant than the rest two dimensions. If layers are too many, this assumption may not be satisfied. This will depend on the type of typical offshore hose, such as length and radius.

8. Parametric analysis

In order to investigate the parameters's effects of reinforcement layers in flexible bonded marine hose, two parameters are controlled in the part which are the internal pressure and winding angle. In offshore engineering, internal pressure are divided into two types: test pressure and working pressure. Normally, working pressure is less than test pressure. Moreover, when the gate of hose suddenly closes, in the hose it is general to appear a vacuum and negative pressure effect. Hence, in the part, three types of internal pressure will be used in parametric analysis.

The winding angle of reinforcement layers are usually ± 55°. However, more winding angles are worth trying to observe the effects on hose itself. In the paper, three winding angles are investigated which are ± 50°,±55°,±60°.

In the above case study, all inputs are suitable for the relatively smaller filament-wound composite pipes. Here a typical flexible bonded marine hose sample is observed, all known quantities of reinforcement

Table 1
Coefficients of the pipe.

Size (mm)		Winding angle (°)		Internal pressure (MPa)
Internal radius	Thickness per layer			
50	0.5	+55(even layer)	−55(odd layer)	10

Table 2
Material constants.

Properties	G_{nn} (GPa)	E (GPa)		ν	
		E_t	E_b	ν_{bt}	ν_{nb}
T300/934	3.88	141.6	10.7	0.268	0.495

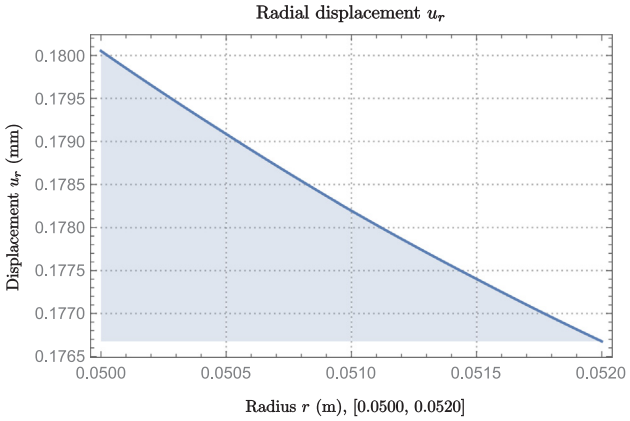

Fig. 7. Displacement in radial direction.

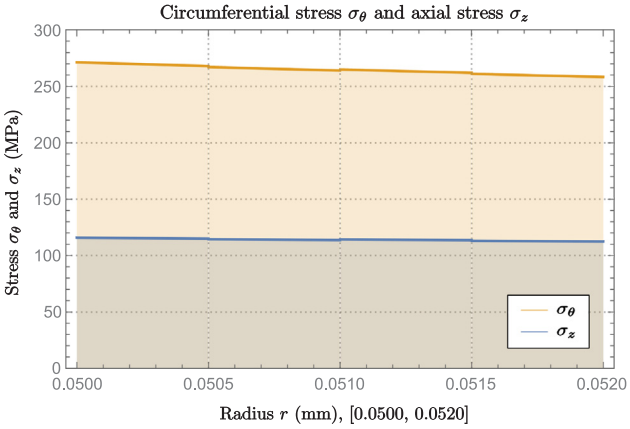

Fig. 8. Circumferential and axial stresses along radius of pipe.

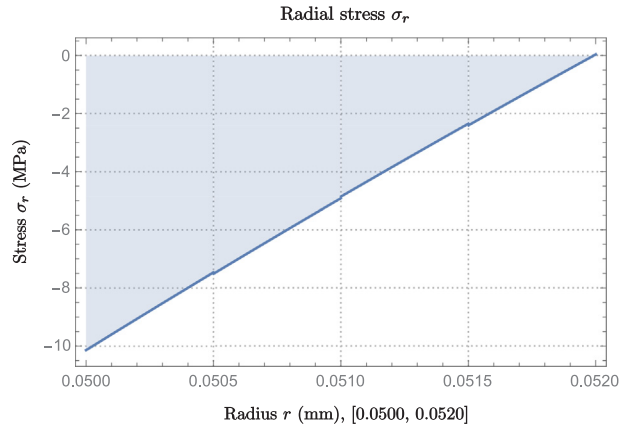

Fig. 9. Shear stress along radius of pipe.

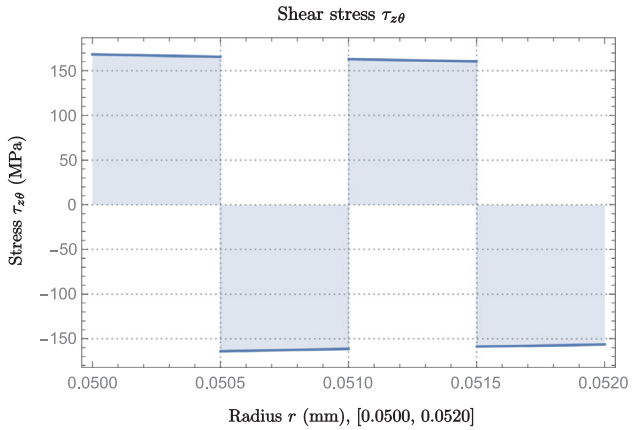

Fig. 10. Shear stress along radius of pipe.

Table 3
Controlled results.

Model	Displacement u_r (mm)	Stresses (MPa)		
		σ_θ	σ_z	$\tau_{z\theta}$
Xia et al. [13]	0.1800	270	118	165
Presented results	0.1800	270	118	165

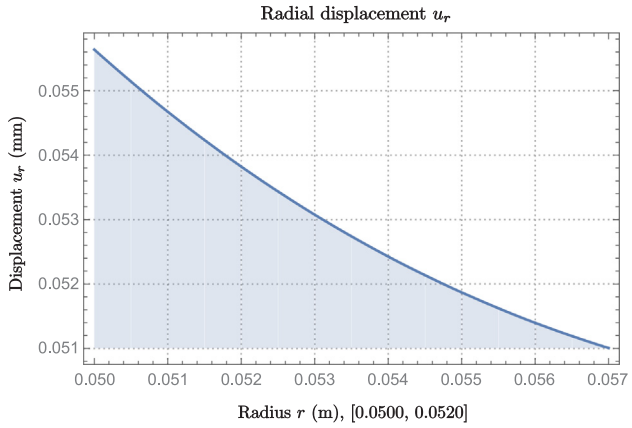

Fig. 11. Displacement in radial direction for 14 layers.

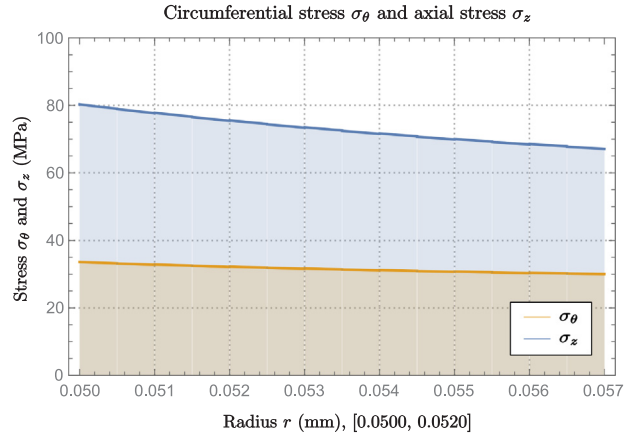

Fig. 12. Circumferential and axial stresses along radius of pipe for 14 layers.

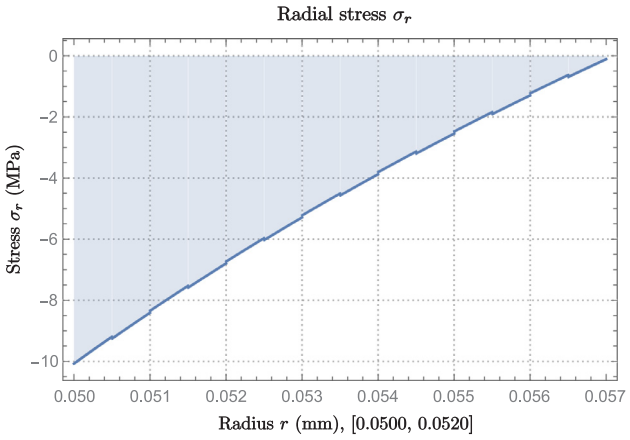

Fig. 13. Shear stress along radius of pipe for 14 layers.

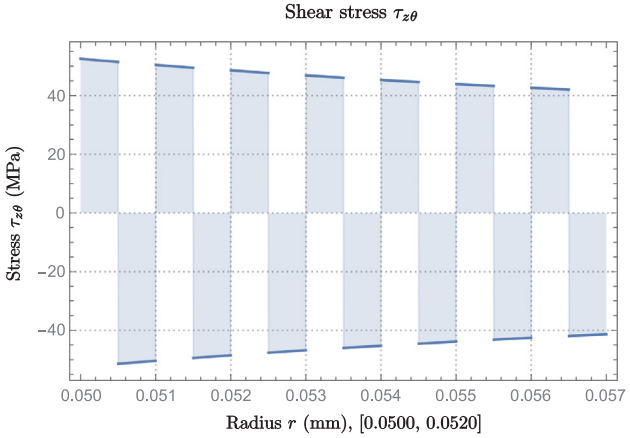

Fig. 14. Shear stress along radius of pipe for 14 layers.

Table 4
Coefficients of reinforcement layers.

Size (mm)		Winding angle (°)			Internal pressure (MPa)		
Internal radius	Thickness per layer				Working	Test	Vacuum
200	1.25	± 45	± 55	± 65	1.5	3.0	−0.085

Table 5
Material constants of reinforcement layers.

Number of layers	G_{nn} (MPa)	E (MPa)		ν	
		E_t	E_b	ν_{bt}	ν_{nt}
14	12.1	384	28.9	0.381	0.476

layers can be listed as follows (Tables 4 and 5):

Since the proposed theoretical method can be operated easily and promptly, all result are convenient to obtained.

8.1. Internal pressure parameterization

Figs. 15 and 16 show the variations of circumferential and axial stresses with respect to radial coordinate, respectively. Three internal pressures are applied to investigate the changes. It can be seen that when internal pressure increases, circumferential and axial stresses both increase proportionally. When the hose exhibits the vacuum and negative pressure effect, the stresses are not significant. Since the

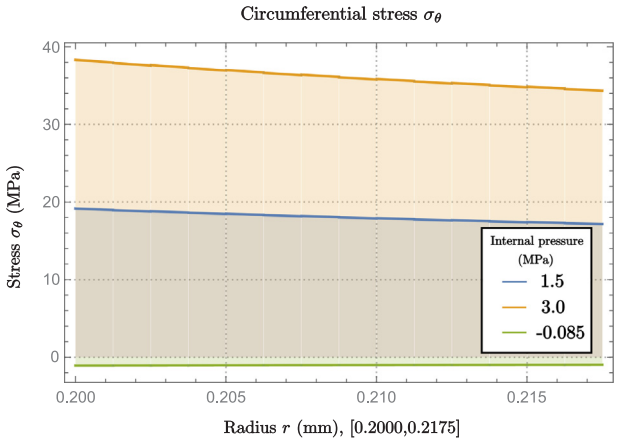

Fig. 15. Circumferential stresses corresponding to 3 internal pressure conditions.

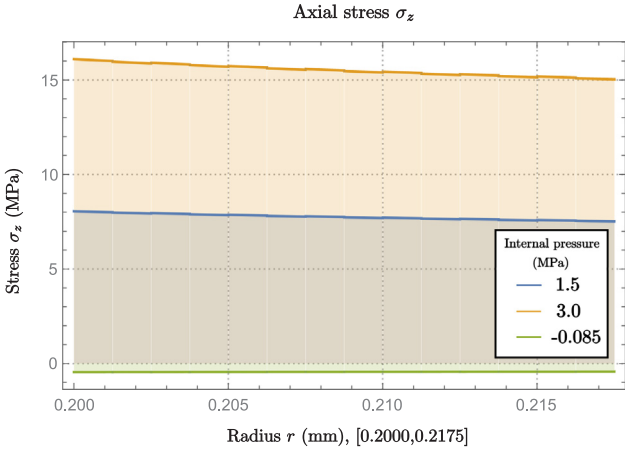

Fig. 16. Axial stresses corresponding to 3 internal pressure conditions.

method proposed in the paper only allows to consider fiber behavior when it works under internal pressure, further investigation including effect of steel coil is in demand to analyze the vacuum and negative pressure conditions.

Fig. 17 can be still considered as a verification for the theoretical method. All radial stresses begin with corresponding initial stress which equals to each internal pressure, and end with zero. Fig. 18 also demonstrates the unified variations of shear stresses when internal pressure changes.

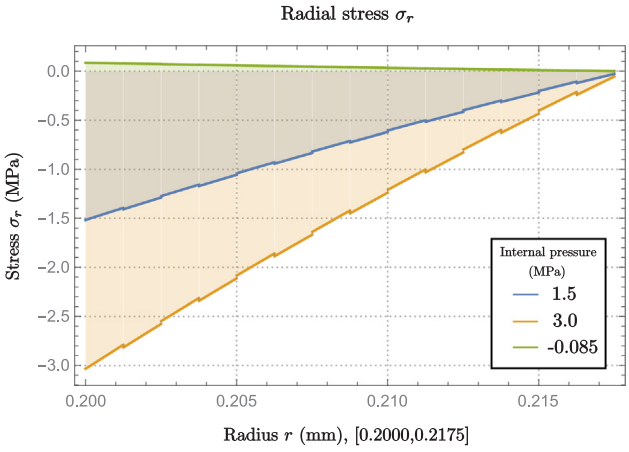

Fig. 17. Radial stresses corresponding to 3 internal pressure conditions.

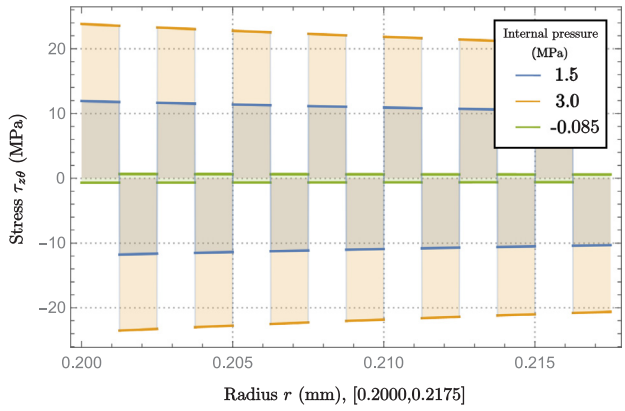

Fig. 18. Shear stresses corresponding to 3 internal pressure conditions.

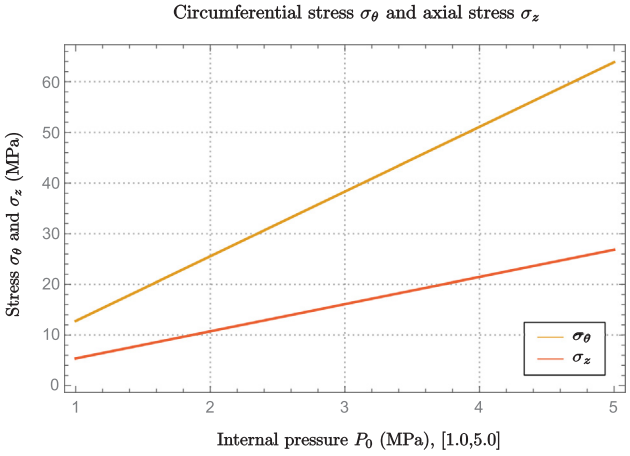

Fig. 19. Circumferential and axial stresses along internal pressure.

All conditions in this part are controlled with a constant ± 55° winding angle since it is the normal winding angle for reinforcement layers in flexible bonded marine hose.

In order to observe the change rate of the stresses corresponding to internal pressure, Fig. 19 depicts the tendency of circumferential and axial stresses along internal pressure from 1.0 MPa to 5.0 MPa. It is of great significance to observe a linear tendency with respect to internal pressure. Namely, based on current theoretical method, the system is linear with respect to internal pressure. The internal pressure should be controlled in a safe range so as to guarantee the normal working condition in offshore engineering.

8.2. Winding angle parameterization

Since the winding angle is a design condition, change rate is therefore not considered in this parametric analysis. Only three winding angles ± 50°,±55°,±60° are investigated. Internal pressure is given by 1.5 MPa, which is the normal working internal pressure.

Fig. 20 shows the variation of circumferential stress with respect to radial coordinate. It is obvious to observe the similar phenomenon as stress corresponding to internal pressure. That is, when winding angle increases, the circumferential stress also significantly increases. The phenomenon can be clearly explained. Since the winding angle is the angle between t – direction and z – direction, if the angle is large enough, this will enhance the whole structure of reinforcement layers. Then it will be more difficult for the structure to stretch along θ – direction. However, it will loose axial stiffness and resistance. The winding angle is better controlled within ± 55°.

Fig. 21 portrays a relatively unique result. All axial stresses are apparently discontinuous, the stress distribution becomes increasingly nonuniform when the winding angle deviates from value ± 55°. Therefore, it can be summarized from the result obtained by the theoretical method that ± 55° would be optimal winding angle for reinforcement layers in marine hose.

According to Fig. 22, it is shown that winding angle plays a inconsequential role in radial stress. However, when winding angle is ± 60°, based on the theoretical method, the curve is disconnected. As the equations mentioned before, the radial stress should be continuous. The figure yields that the proposed theoretical method is not perfectly applicable for large winding angle conditions with respect to radial stress. The precision will remarkably deteriorated with increasing of the winding angle.

As is shown is Fig. 23, the shear stresses corresponding to 3 winding angle conditions is still legitimate. The shear stress will increase when winding angle increases. However, from the figure it can be seen that the change rate is not constant.

8.3. Results for different number of layers

Results of three kinds of stresses along internal radius corresponding to different number of layers are presented below in Fig. 24. The condition is under a typical 1.5 MPa internal pressure. Since the method proposed to be generic, different number of layers can be also listed as a parametric condition to show the change of all mechanical results.

From Fig. 24, circumferential, axial and shear stresses show similar decreases corresponding to different fiber layers, since it is more difficult for the structure to stretch with the increase of layers. However, a lesser decrease extent is observed from the three obtained curves, which means that the influence made by the number of layers is in decline. Although theoretically the optimal number of reinforcement layers which can be observed in the figure confirms to be infinite, it can be concluded that an appropriate number of reinforcement layers which combines validity and economy is preferential to be recommended in structural design of reinforcement layers in offshore hoses.

8.4. Parametric comparison with experimental results

In Ref. [15], an experimental test is applied for an sample of lament-wound fiber-reinforced composite pipe. The material is determined with resin (UE-5210). The internal radius is 50 mm while external radius is 74 mm. The length of the pipe is 900 mm. The properties of the sample are provided in [15]. To make a contrast, here considering the experimental results of axial and circumferential strains measured in central part of the pipe along axial and circumferential directions, the compared studies are presented in Figs. 25 and 26.

The results portrays the changing of strains per unit of internal pressure (MPa) corresponding to different winding angles. From the

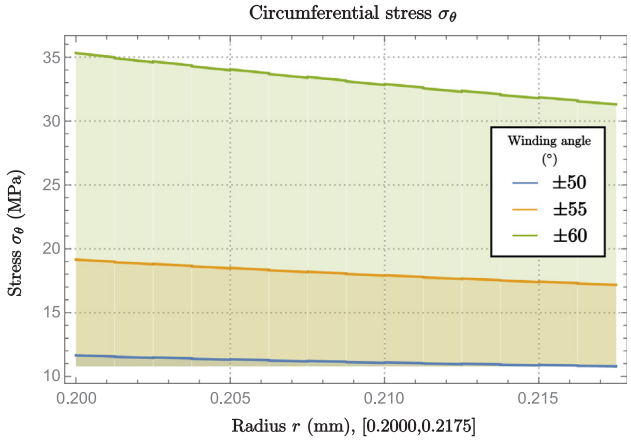

Fig. 20. Circumferential stresses corresponding to 3 winding angle conditions.

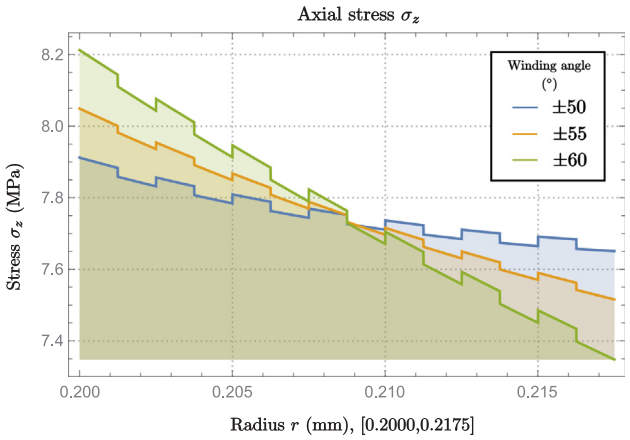

Fig. 21. Axial stresses corresponding to 3 winding angle conditions.

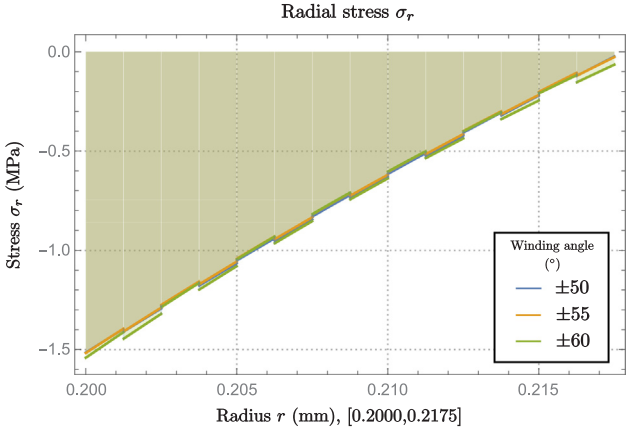

Fig. 22. Radial stresses corresponding to 3 winding angle conditions.

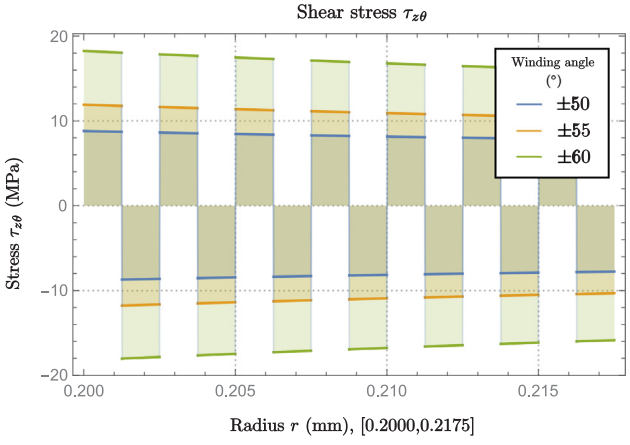

Fig. 23. Shear stresses corresponding to 3 winding angle conditions.

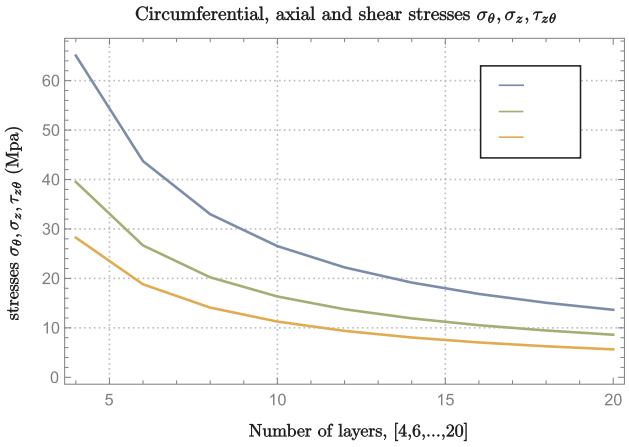

Fig. 24. Stresses corresponding to different layers (4, 6, …, 20).

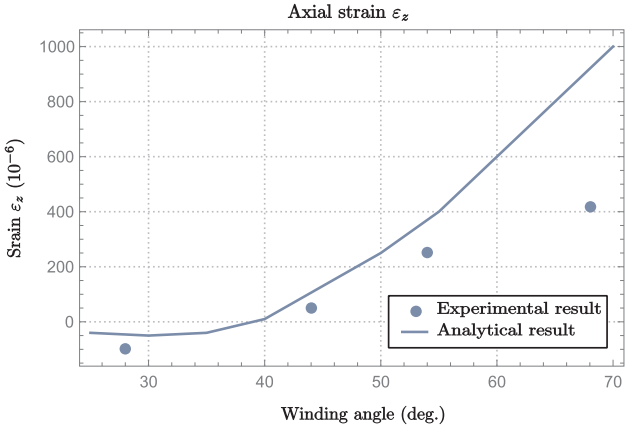

Fig. 25. Comparison of axial strain ε_z with experimental results.

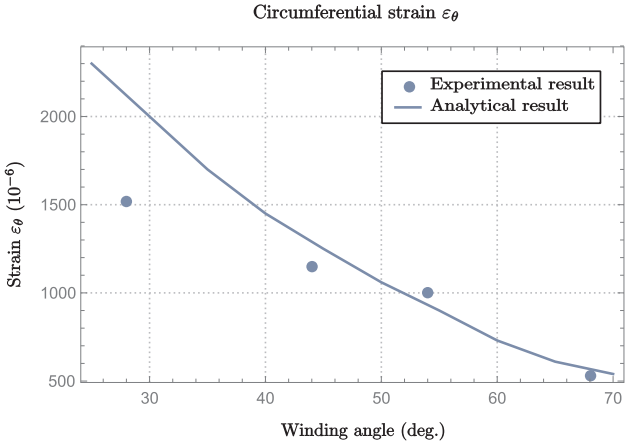

Fig. 26. Comparison of circumferential strain ε_θ with experimental results.

figures, not only the influence made by winding angle on different strains can be observed, but also the comparisons between analytical and experimental results are revealed.

As is shown in Figs. 25 and 26, the axial strain increases with respect to increasing of winding angle while the circumferential strain is the opposite. At the range of winding angle from 45° to 45°, good correlations between analytical and experimental results can be observed. However, when winding angle is big enough, the experimental results of axial strain ε_z are significant smaller than analytical results. On the contrary, the significant difference of circumferential strain ε_θ between experimental and analytical results occurs while the winding angle is quite small.

These tendencies are related to the directions of strains. For instance, when winding angle is too big, from analytical solution it can be inferred that the material is more likely to stretch along axial strain, which is not always satisfied in experimental test due to instability of the actual samples. These compared results are also in accordance with that in Ref. [15].

8.5. Parametric comparison with FE model

In this part, parametric comparison with FE model in Ref. [2] is

given. Note that, Ref. [2] includes both axisymmetric and 3D full models for global offshore hoses, as well as experimental results for burst pressure. However, the proposed analytical model can be applicable only in reinforcement plies, other layers which will also show influence on the final results such as steel coil are not included in the analytical model. Although the results may not reach agreement perfectly, comparison between models is still important to demonstrate the uncertainties and limits of the proposed analytical method, as well as for having a clear view of the merits and demerits.

In Ref. [2], the material properties of reinforcement layers can be derived by load vs. strain curves of the cords. The numerical results of burst pressure predictions given by the axisymmetric and 3D models were obtained based on radial displacement corresponding to internal pressure. Considering that the differences between axisymmetric and 3D models are not too much, comparison between the proposed analytical results and axisymmetric numerical results are analyzed.

In this case, a typical double carcass structure with 46 (20 + 10 + 16) reinforcement plies and one steel coil is chosen as the typical sample. To make a contrast, the theoretical model of a consecutive 46 layered reinforcement structure is considered. Using the known quantities provided in Ref. [2], the comparison result of radius displacements u_r is given in Fig. 27.

Since only the burst pressure is observed in experimental test, one experimental result of 14 MPa which is the burst pressure of the whole hose is given in Fig. 27. The variation of radial displacement u_r before burst pressure predicted from analytical analysis and finite element analysis are also presented. The derivations between two different methods increase with respect to internal pressure, which could be explained by the different structure assembly and the influence made by steel coil. Non-linearity effects related to hyperelastic behavior of rubber layers also bring some errors. In finite element model, after 11 MPa internal pressure, plastic strain phenomenon occurs, which will force the displacement to increase faster, until the burst pressure. Hence, until now it still cannot observe this phenomenon and further burst pressure prediction in the present analytical model due to the linear results of radial displacement corresponding to internal pressure.

However, the differences between analytical and finite element results from the beginning of internal pressure are not significant, which shows that the steel coil plays an inconsequential role in providing radial protection compared to reinforcement layers when internal pressure is not significant. Therefore, under general internal pressure condition, the analytical model can be a rudimentary replacement to predict the radial behavior of the whole hose structure.

9. Failure analysis

In offshore engineering, failure analysis is a key component of scientific research. To validate the design load of reinforcement layers in flexible bonded marine hose, it is significant to investigate and check the utilization factor of each layer in flexible bonded marine hose.

According to API 17 K [3], the design criteria for reinforcement layers is mechanical load. Under service condition and normal operation, the permissible utilization factor is provided as 0.55. Hence, the key task is to find the largest mechanical load in reinforcement layers. Considering the corresponding failure criterion, the utilization factor can be obtained.

Based on previous discussion, it is concluded that the largest stress always appears in the first reinforcement layer. The stresses can be extruded in previous data corresponding to internal radius (r = 200 mm).

Normally, there are five types failure criteria, which are maximum stress failure criterion, maximum strain failure criterion, Tsai-Hill failure criterion, Hoffman failure criterion and Tsai-Wu tensor failure criterion. Since Tsai-Hill failure criterion appears to be more applicable to failure prediction for composite material than either maximum stress criterion or maximum strain failure criterion, and the composite material is considered ductile, the latter two criteria are not adopted in the case.

Moreover, due to same strengths in tension and compression in the studied composite material, Tsai-Hill failure criterion is enough to analyze the failure mode, since Hoffman failure criterion and Tsai-Wu tensor failure criterion are both suitable for different strengths in tension and compression.

The Tsai-Hill failure criterion can be demonstrated as follows:

$$\frac{\sigma_1^2}{X^2}-\frac{\sigma_1\sigma_2}{X^2}+\frac{\sigma_2^2}{Y^2}+\frac{\tau_{12}^2}{S^2}=1 \tag{41}$$

where X,Y,S represent the lamina principal strengths. Considering the recommended principal strengths of reinforcement layers in flexible bonded marine hose (internal radius r = 200 mm), these values can be given by

$$X=317,\quad Y=15,\quad S=6 \tag{42}$$

The left side of the equation which is the discriminant must be less than the permissible utilization factor (normally 1, here 0.55); otherwise, fracture is said to have occurred.

Moreover, the stress results given by the proposed theoretical method are stresses along cylindrical coordinate. To calculate the value of the discriminant, the stress results are therefore transformed to stresses along standard coordinate (x,y,z):

$$\begin{bmatrix}\sigma_1\\ \sigma_2\\ \tau_{12}\end{bmatrix}=\begin{bmatrix}\sigma_x\\ \sigma_y\\ \tau_{xy}\end{bmatrix}=\begin{bmatrix}m^2 & n^2 & 0 & 0 & 0 & 2mn\\ n^2 & m^2 & 0 & 0 & 0 & -2mn\\ -mn & mn & 0 & 0 & 0 & m^2-n^2\end{bmatrix}\begin{bmatrix}\sigma_z\\ \sigma_\theta\\ \sigma_r\\ \tau_{\theta r}\\ \tau_{zr}\\ \tau_{z\theta}\end{bmatrix} \tag{43}$$

where $m=\cos\phi$,$n=\sin\phi$. ϕ is the winding angle.

Then, σ_1,σ_2,τ_{12} can be calculated. Considering three practical internal pressure conditions, all check results can be listed in the following table (Table 6):

From the table provided above, it can be seen that the utilization of reinforcement layers is relatively low with respect to low internal pressure. Three types of internal pressure are capable for utilization check. However, if internal pressure is over 3.0 MPa, the utilization factor may exceed the permissable utilization limit. It can be concluded that working condition is safe enough for offshore engineering, and test condition can be an essential reference for experimental check of reinforcement samples in flexible bonded marine hose.

10. Conclusion

This paper presents a general analysis of reinforcement layers in bonded flexible marine hoses under internal pressure. A theoretical

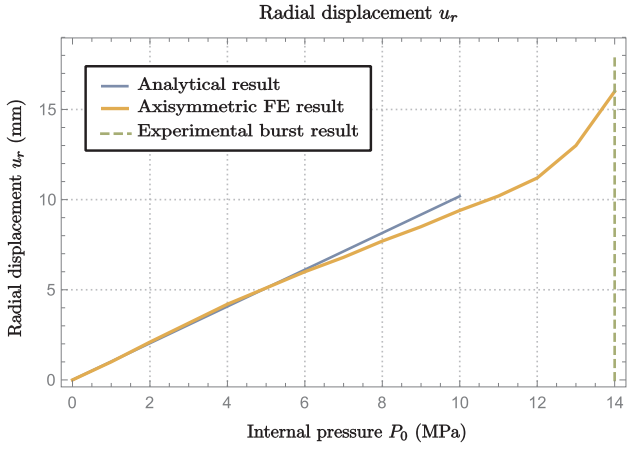

Fig. 27. Comparison of radial displacement with Ref. [2].

Table 6
Reinforcement layers utilization check.

Internal pressure	σ_1	σ_2	τ_{12}	X	Y	S	Utilization	permissible	Check result
1.5MPa	26.70	0.51	1.14	317	15	6	0.04	<0.55	√
3.0MPa	53.40	1.01	2.29	317	15	6	0.18	<0.55	√
−0.085MPa	−1.51	−0.03	−0.06	317	15	6	1.43×10^{-4}	<0.55	√

solution based on anisotropic laminated composite model is established. The final solver is determined with a unified linear equation system derived from an existing model from Xia et al. [13] which can be applicable for any number of layered composite laminates. Consequently, the mechanical model of a reinforcement structure in marine hoses can be solved analytically. Through the case study including stress and strain analysis compared with previous paper, a sound theory of reinforcement layers in bonded flexible marine hoses that accords with industrial requirements is substantiated. Moreover, a 14-layered reinforcement structure is explored and discussed. The provided results enable a preliminary examination of reinforcement fiber layers which can provide reliable guidance for further design and verification of global behaviour of marine hoses.

Parametric analysis and failure analysis are also investigated. Combining differential internal pressure, winding angle conditions and different number of layers, more new results are obtained. An optimal ± 55° winding angle is convinced. Due to concise programming implementation, these post-processing results can be concluded efficiently after only one calculating process.

Although all results presented in the paper can be valid references for practical construction, some engineering factors still remain uncertain. Further studies are necessary to consider the mechanical behaviour of rebar layer since this is also significant in representing the polymeric reinforcement. More boundary conditions such as bending and tension should be included. All factors mentioned above definitely open up the possibility in comparison with various finite element results in marine hoses study in the future.

Acknowledgements

This work is financially supported by China National Key Research and Development Plan (Grant No. 2016YFC0303704) and National Natural Science Foundation of China (Grant No. 51509258). The authors also gratefully acknowledge Heibei Jingxian Zebang Rubber Technology, Co., Ltd for the financial support.

Appendix A

The matrix formula of $[A_{pi}]$ is as follows:

$$[A_{pi}] = \begin{bmatrix} m^4 & n^4 & 0 & 2m^2n^2 & 0 & 0 & 0 & 0 & 4m^2n^2 \\ m^2n^2 & m^2n^2 & 0 & m^4+n^4 & 0 & 0 & 0 & 0 & -4m^2n^2 \\ 0 & 0 & 0 & 0 & m^2 & n^2 & 0 & 0 & 0 \\ m^3n & -mn^3 & 0 & -m^3n+mn^3 & 0 & 0 & 0 & 0 & -2m^3n+2mn^3 \\ n^4 & m^4 & 0 & 2m^2n^2 & 0 & 0 & 0 & 0 & 4m^2n^2 \\ 0 & 0 & 0 & 0 & n^2 & m^2 & 0 & 0 & 0 \\ mn^3 & -m^3n & 0 & m^3n-mn^3 & 0 & 0 & 0 & 0 & 2m^3n-2mn^3 \\ 0 & 0 & 1 & 0 & 0 & 0 & 0 & 0 & 0 \\ 0 & 0 & 0 & 0 & mn & -mn & 0 & 0 & 0 \\ 0 & 0 & 1 & 0 & 0 & 0 & m^2 & n^2 & 0 \\ 0 & 0 & 1 & 0 & 0 & 0 & -mn & mn & 0 \\ 0 & 0 & 1 & 0 & 0 & 0 & n^2 & m^2 & 0 \\ m^2n^2 & m^2n^2 & 0 & -2m^2n^2 & 0 & 0 & 0 & 0 & (m^2-n^2)^2 \end{bmatrix} \tag{A.1}$$

where $m = \cos\phi, n = \sin\phi$. ϕ is the winding angle.

The expressions of elements in matrices $\boldsymbol{A}$,$\boldsymbol{B}$ and $\boldsymbol{\Lambda}$ are as follows:

$\boldsymbol{A}$:

$$a_{ij} = \begin{cases} (C_{23}^{(j)} + \alpha^{(j)} C_{33}^{(j)}) r_{j-1}^{\alpha^{(j)}-1}, & i = j = 1 \\ r_j^{\alpha^{(j)}}, & i = j+1 = 2,\ldots,N \\ -r_{j-1}^{\alpha^{(j)}}, & i = j = 2,\ldots,N \\ (C_{23}^{(j)} + \alpha^{(j)} C_{33}^{(j)}) r_j^{\alpha^{(j)}-1}, & i = j+N = N+1,\ldots,2N \\ -(C_{23}^{(j)} + \alpha^{(j)} C_{33}^{(j)}) r_{j-1}^{\alpha^{(j)}-1}, & i = j+N-1 = N+1,\ldots,2N-1 \\ \frac{C_{12}^{(j)} + \alpha^{(j)} C_{13}^{(j)}}{1+\alpha^{(j)}} (r_j^{\alpha^{(j)}+1} - r_{j-1}^{\alpha^{(j)}+1}), & i = 2N+1, j = 1,\ldots,N \\ \frac{C_{26}^{(j)} + \alpha^{(j)} C_{36}^{(j)}}{2+\alpha^{(j)}} (r_j^{\alpha^{(j)}+2} - r_{j-1}^{\alpha^{(j)}+2}), & i = 2N+2, j = 1,\ldots,N \end{cases} \tag{A.2}$$

$\boldsymbol{B}$:

$$b_{ij} = \begin{cases} (C_{23}^{(j)} - \alpha^{(j)} C_{33}^{(j)}) r_{j-1}^{-\alpha^{(j)}-1}, & i = j = 1 \\ r_j^{-\alpha^{(j)}}, & i = j+1 = 2,...,N \\ -r_{j-1}^{-\alpha^{(j)}}, & i = j = 2,...,N \\ (C_{23}^{(j)} - \alpha^{(j)} C_{33}^{(j)}) r_j^{-\alpha^{(j)}-1}, & i = j+N = N+1,...,2N \\ -(C_{23}^{(j)} - \alpha^{(j)} C_{33}^{(j)}) r_{j-1}^{-\alpha^{(j)}-1}, & i = j+N-1 = N+1,...,2N-1 \\ \frac{C_{12}^{(j)} - \alpha^{(j)} C_{13}^{(j)}}{1-\alpha^{(j)}} (r_j^{-\alpha^{(j)}+1} - r_{j-1}^{-\alpha^{(j)}+1}), & i = 2N+1, j = 1,...,N \\ \frac{C_{26}^{(j)} - \alpha^{(j)} C_{36}^{(j)}}{2-\alpha^{(j)}} (r_j^{-\alpha^{(j)}+2} - r_{j-1}^{-\alpha^{(j)}+2}), & i = 2N+2, j = 1,...,N \end{cases} \tag{A.3}$$

Λ:

$$\lambda_{k1} = \begin{cases} C_{13}^{(k)} + \beta_2^{(k)} (C_{23}^{(k)} + C_{33}^{(k)}), & k = 1 \\ (\beta_2^{(k-1)} - \beta_2^{(k)}) r_{k-1}, & k = 2,...,N \\ (C_{13}^{(k-N)} - C_{13}^{(k-N+1)}) + (C_{23}^{(k-N)} + C_{33}^{(k-N)}) \beta_2^{(k-N)} - (C_{23}^{(k-N+1)} + C_{33}^{(k-N+1)}) \beta_2^{(k-N+1)}, & k = N+1,...,2N-1 \\ C_{13}^{(k/2)} + \beta_2^{(k/2)} (C_{23}^{(k/2)} + C_{33}^{(k/2)}), & k = 2N \end{cases} \tag{A.4}$$

$$\begin{aligned} \lambda_{(2N+1)1} &= \sum_{k=1}^{N} [C_{11}^{(k)} + \beta_2 (C_{12}^{(k)} + C_{13}^{(k)})] \frac{(r_k^2 - r_{k-1}^2)}{2} \\ \lambda_{(2N+2)1} &= \sum_{k=1}^{N} [C_{16}^{(k)} + \beta_2 (C_{26}^{(k)} + C_{36}^{(k)})] \frac{(r_k^3 - r_{k-1}^3)}{3} \end{aligned} \tag{A.5}$$

$$\lambda_{k2} = \begin{cases} [C_{36}^{(k)} + \beta_1 (C_{23}^{(k)} + 2C_{33}^{(k)})] r_{k-1}, & k = 1 \\ (\beta_1^{(k-1)} - \beta_1^{(k)}) r_{k-1}^2, & k = 2,...,N \\ [(C_{36}^{(k-N)} - C_{36}^{(k-N+1)}) + (C_{23}^{(k-N)} + 2C_{33}^{(k-N)}) \beta_1^{(k-N)} - (C_{23}^{(k-N+1)} + 2C_{33}^{(k-N+1)}) \beta_1^{(k-N+1)}] r_{k-N}, & k = N+1,...,2N-1 \\ [C_{36}^{(k/2)} + \beta_1^{(k/2)} (C_{23}^{(k/2)} + 2C_{33}^{(k/2)})] r_{k/2}, & k = 2N \end{cases} \tag{A.6}$$

$$\begin{aligned} \lambda_{(2N+1)2} &= \sum_{k=1}^{N} [C_{16}^{(k)} + \beta_1 (C_{12}^{(k)} + 2C_{13}^{(k)})] \frac{(r_k^3 - r_{k-1}^3)}{3} \\ \lambda_{(2N+2)2} &= \sum_{k=1}^{N} [C_{66}^{(k)} + \beta_1 (C_{26}^{(k)} + 2C_{36}^{(k)})] \frac{(r_k^4 - r_{k-1}^4)}{4} \end{aligned} \tag{A.7}$$

References

[1] Gonzalez GM, de Sousa JR, Sagrilo LV. A study on the axial behavior of bonded flexible marine hoses. Mar Syst Ocean Technol 2016;11(3–4):31–43.

[2] Tonatto MLP, Tita V, Araujo RT, Forte MMC, Amico SC. Parametric analysis of an offloading hose under internal pressure via computational modeling. Mar Struct 2017;51:174–87.

[3] API. API 17K, Specification for bonded flexible pipes. Washington (DC): API Publishing Services; 2001.

[4] OCIMF. Guide to purschasing, manufacturing and testing of loading and discharge hoses for offshore moorings. Londres: Witherbyd & CO. LTDA; 2009.

[5] Northcutt VM. Bonded flexible pipe. In: OCEANS 2000 MTS/IEEE conference and exhibition, vol. 2. IEEE; 2000. p. 1407–12.

[6] Lassen T, Eide AL, Meling TS. Ultimate strength and fatigue durability of steel reinforced rubber loading hoses. In: ASME 2010 29th international conference on ocean, offshore and arctic engineering. American Society of Mechanical Engineers; 2010. p. 277–86.

[7] Lassen T, Lem AI, Imingen G. Load response and finite element modelling of bonded loading hoses. In: ASME 2014 33rd international conference on ocean, offshore and arctic engineering. American Society of Mechanical Engineers; 2014. p. V06AT04A034–V06AT04A034.

[8] Batista RC, Bogarin JA, Ebecken NF. Local mechanical behaviour of multilayered flexible risers. In: Proceedings of the 7th international symposium on offshore engineering; 1989. p. 494–510.

[9] Rosenow M. Wind angle effects in glass fibre-reinforced polyester filament wound pipes. Composites 1984;15(2):144–52.

[10] Wild P, Vickers G. Analysis of filament-wound cylindrical shells under combined centrifugal, pressure and axial loading. Compos Part A: Appl Sci Manuf 1997;28(1):47–55.

[11] Smerdov A. A computational study in optimum formulations of optimization problems on laminated cylindrical shells for buckling I. Shells under axial compression. Compos Sci Technol 2000;60(11):2057–66.

[12] Smerdov A. A computational study in optimum formulations of optimization problems on laminated cylindrical shells for buckling II. Shells under external pressure. Compos Sci Technol 2000;60(11):2067–76.

[13] Xia M, Takayanagi H, Kemmochi K. Analysis of multi-layered filament-wound composite pipes under internal pressure. Compos Struct 2001;53(4):483–91.

[14] Xia M, Takayanagi H, Kemmochi K. Bending behavior of filament-wound fiber-reinforced sandwich pipes. Compos Struct 2002;56(2):201–10.

[15] Takayanagi H, Xia M, Kemmochi K. Stiffness and strength of filament-wound fiber-reinforced composite pipes under internal pressure. Adv Compos Mater 2002;11(2):137–49.

[16] Ansari R, Alisafaei F, Ghaedi P. Dynamic analysis of multi-layered filament-wound composite pipes subjected to cyclic internal pressure and cyclic temperature. Compos Struct 2010;92(5):1100–9.

[17] Sayman O. Analysis of multi-layered composite cylinders under hygrothermal loading. Compos Part A: Appl Sci Manuf 2005;36(7):923–33.

[18] Bakaiyan H, Hosseini H, Ameri E. Analysis of multi-layered filament-wound composite pipes under combined internal pressure and thermomechanical loading with thermal variations. Compos Struct 2009;88(4):532–41.

[19] Landau L, Lifshitz E. Theory of elasticity. 3rd ed.; 1986.

[20] Abraham R, Marsden JE, Ratiu T. Manifolds, tensor analysis, and applications vol. 75. Springer Science & Business Media; 2012.